ResearchGate

See discussions, stats, and author profiles for this publication at: https://www.researchgate.net/publication/3131333

Two-resonator method for measurement of dielectric anisotropy in multilayer samples

Article *in* IEEE Transactions on Microwave Theory and Techniques · July 2006

DOI: 10.1109/TMTT.2006.871247 · Source: IEEE Xplore

CITATIONS
57

READS
535

1 author:

Plamen Dankov
Sofia University "St. Kliment Ohridski"

153 PUBLICATIONS **301** CITATIONS

SEE PROFILE

Some of the authors of this publication are also working on these related projects:

Project MODELING, SIMULATION, COMPUTER-AIDED DESIGN, AND OPTIMIZATION OF GYROTRONS View project

All content following this page was uploaded by Plamen Dankov on 14 August 2014.

The user has requested enhancement of the downloaded file.

Two-Resonator Method for Measurement of Dielectric Anisotropy in Multilayer Samples

Plamen I. Dankov, *Member, IEEE*

***Abstract*—A two-resonator method, based on TE_{011}-mode and TM_{010}-mode resonance cavities with a multilayer disk sample, has been developed for measurements of the longitudinal and transversal dielectric constant and dielectric loss tangent of each layer (if the other ones have known parameters) or in the whole sample averaging over the layers contribution. Dispersion equations for the considered modes in both types of cavities with three-, two-, or one-layer samples are obtained. The measurement sensitivity and errors in the dielectric constant are discussed. Analytical expressions for the computation of the dielectric loss tangent of the unknown layer in the two directions are presented for each of the considered cavities. The proposed method is applicable in simple laboratory conditions and allows an estimation of the dielectric anisotropy of multilayer materials in many practical cases. The measuring errors for one-layer artificial substrates with thicknesses of 0.25–0.5 mm are approximately 3%–6% for dielectric constants in the interval of 2.0–4.5 and 10%–15% for dielectric loss tangents in the interval of 0.002–0.010. The obtained pair of longitudinal and transversal dielectric parameters can be used in modern structure simulators for more realistic simulations of microwave components, radiating elements, antenna radomes, etc. Three practical examples for three-layer antenna radomes are given for an illustration of the dielectric anisotropy characterization of multilayer samples.**

***Index Terms*—Anisotropic media, cavity resonators, dielectric losses, multilayers, permittivity measurement, radomes.**

I. INTRODUCTION

IT IS a known fact that the successful design of many planar passive or active devices with microwave simulators is very sensitive upon the values of relative dielectric constant ε_r and dielectric loss tangent $\tan\delta_\varepsilon$ of the materials: substrates, thin films, multilayer composites, etc. used in the simulations. The catalog data usually obtained by the IPC TM-650 2.5.5.5 stripline-resonator test method [1] include parameters $\varepsilon'_\perp$ and $\tan\delta_{\varepsilon\perp}$ (near-to-transversal values, i.e., normal to the substrate surface), but this may be insufficient in many design cases. It is known that designers "tune" the dielectric constant about the known catalog values in order to fit simulated and measured dependencies for a designed device. The problem appears when the substrates have a noticeable dielectric anisotropy, i.e., different values of the longitudinal and transversal dielectric constant ($\varepsilon'_\parallel \neq \varepsilon'_\perp$ [2]) or of the dielectric loss tangent ($\tan\delta_{\varepsilon\parallel} \neq \tan\delta_{\varepsilon\perp}$—see denotations in Fig. 1). We established in [3] and [4] using the perturbation technique that most of the commercial reinforced laminates (with layers of woven glass, ceramic powders, organic filling, etc.) have a noticeable dielectric anisotropy (e.g., up to 15%–25% for dielectric constant anisotropy $\Delta A_\varepsilon = 2|\varepsilon'_\parallel - \varepsilon'_\perp|/(\varepsilon'_\parallel + \varepsilon'_\perp)$ and up to 50%–80% for dielectric loss tangent anisotropy $\Delta A_{\tan\delta\varepsilon} = 2|\tan\delta_{\varepsilon\parallel} - \tan\delta_{\varepsilon\perp}|/(\tan\delta_{\varepsilon\parallel} + \tan\delta_{\varepsilon\perp})$. This problem could be partially overcome if an equivalent dielectric constant $\varepsilon'_{\mathrm{eq}}$ is introduced as in [5] (and similarly for $\tan\delta_{\varepsilon\mathrm{eq}}$, as in [4]), which transforms the real anisotropic microstrip structure into an equivalent isotropic one. The usefulness of the equivalent parameters ($\varepsilon'_{\mathrm{eq}}$, $\tan\delta_{\varepsilon\mathrm{eq}}$) depends on the device structure and is restricted to transmission lines with non-TEM propagation modes (e.g., coplanar waveguides), multiimpedance structures, and RF components, which support high-order modes like T-junctions, steps, stubs, gaps, etc. [4]. The multilayer materials are used in many practical cases, which are, in principle, anisotropic samples: bonded (with pre-preg films) substrates in multilayer antenna panels, thin absorbing nanoparticle films on supporting tapes [6], composite antenna radomes [7], etc.

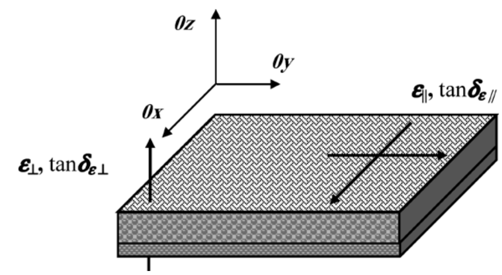

Fig. 1. Two pairs of longitudinal (in the $x0y$-plane) and transversal (along the $0z$-axis) dielectric parameters in multilayer anisotropic substrate.

In this paper, we developed the *two-resonator method* proposed in [8] for the characterization of the dielectric anisotropy ΔA_ε and $\Delta A_{\tan\delta\varepsilon}$ in planar multilayer samples. Two different cylindrical resonators are used for this purpose, which support two suitable azimuthally symmetrical modes—the TE_{011} mode for the determination of $\varepsilon'_\parallel$, $\tan\delta_{\varepsilon\parallel}$ and the TM_{010} mode—for $\varepsilon'_\perp$, $\tan\delta_{\varepsilon\perp}$.

The idea to use TE_{011}- and TM_{010}-mode resonators for complex dielectric constant measurements is not new. Several cavity-resonator methods for a low-loss dielectric property characterization have been presented in the literature (e.g., see a useful comparison in [9]). Most of them are accepted in metrology institutions like the National Institute of Standards and Technology (NIST), Boulder, CO [10] and the National Physics

Manuscript received September 21, 2005; revised December 12, 2005. This work was supported in part by the National Innovation Fund in Bulgaria and by Elco-Star Com Ltd. under Contract IF-00-160/28.10.2005.

The author is with the Faculty of Physics, Department of Radio-Physics and Electronics, University of Sofia, 1164-Sofia, Bulgaria (e-mail: dankov@phys.uni-sofia.bg).

Digital Object Identifier 10.1109/TMTT.2006.871247

0018-9480/$20.00 © 2006 IEEE

Laboratory (NPL), Middlesex, U.K. [11] for reference methods, but for isotropic materials as a rule. However, there is no universal solution for the dielectric anisotropy measurements. Usually, the parameters $\varepsilon'_{\|}$ and $\tan\delta_{\varepsilon\|}$ can be measured using TE-mode resonance cavities (classical Courtney's method [12], Kent's evanescent-mode tester [13], NIST's mode-filtered resonator [14], split-cylinder resonator [15], etc.). The parameters $\varepsilon'_{\perp}$ and $\tan\delta_{\varepsilon\perp}$ can be estimated using TM-mode resonance cavities [16], low-frequency reentrant cavities [17], etc. In fact, only a few publications have been directly dedicated to dielectric-anisotropy measurements. Whispering-gallery modes in single dielectric resonators could be used for anisotropy measurement of ultra and extremely low-loss materials [18]–[20]. A split-cavity method for the dielectric-constant anisotropy determination through a long cylindrical cavity with TE_{111} and $\mathrm{TM}_{\mathrm{nm}0}$ modes is described in [21] and data for some reinforced materials are presented.

The aim of our investigations is to present a workable and relatively universal method based on simple laboratory equipment for measurements of the dielectric anisotropy of *one* dielectric sample using *two* cavity resonators. Thus, variations of properties from sample to sample could be avoided. Each of the considered measuring resonators is designed to ensure the best excitation conditions for necessary azimuthally symmetrical TE or TM modes. Resonance cavities with one-, two-, and three-layer samples are considered covering most of the practical cases. The proposed method allows easily estimation of the dielectric parameters of anisotropic multilayer materials with two options: separately in every layer or in the whole sample averaging over the layers ("average" sample). The measured pairs of values ($\varepsilon'_{\|}$ and $\varepsilon'_{\perp}$, $\tan\delta_{\varepsilon\|}$ and $\tan\delta_{\varepsilon\perp}$) can be used in microwave simulators for more accurate simulations during the design process.

II. Two Resonance Cylindrical Cavities With MultiLayer Samples

The theory of the proposed method concerning the calculation of the dielectric constant and dielectric loss tangent of multilayer samples is presented below.

A. *Dispersion Equations for the Determination of the Dielectric Constant in Multilayer Samples*

A five-layer resonance cavity is represented in Fig. 2, where the parameters of the layers are denoted. One dielectric film/layer (1) is placed between two dielectric supporting layers (2, 3), while the other two parts (4, 5) are foam (or air) filled. Two different resonance cavities are proposed for the determination of the dielectric constants in two directions—along the resonator axis and perpendicularly to it. When a sandwich-type disk sample (layers 1–3) is placed in the resonator half-height $H/2$, the excited TE_{011} mode in the resonance cavity (R1) can be used for the determination of the longitudinal dielectric constant $\varepsilon'_{\|}$ of the sample. This is because the electric field is orientated along its surfaces and it has its maximum at $H/2$—cases in Fig. 3(a). It is better in these cases to choose an equal resonator diameter and height $D \cong H(= h_1+h_2+h_3+h_4+h_5)$ in order to separate the TE_{011} mode from the other low-

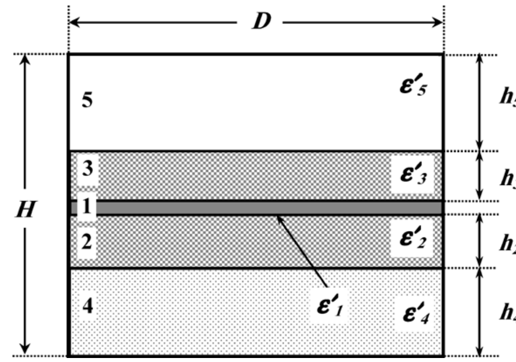

Fig. 2. Layers in the resonance cavity. 1: Unknown dielectric layer. 2,3: Two supporting dielectric layers. 4, 5: Foam (or air)-filled parts (not to scale).

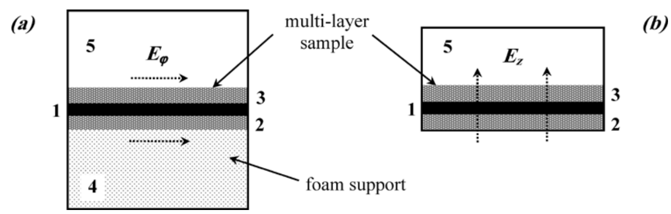

Fig. 3. Two types of measuring cavities. (a) TE_{011}-mode cavity ($\mathbf{R1}$). (b) TM_{010}-mode cavity ($\mathbf{R2}$) ($h_4 = 0$). Both with three-layer samples. The arrows denote the predominant direction of the electric field of the corresponding mode at the resonance.

and high-order modes (see [3]). The other type of resonator (R2) is designed to support the TM_{010} mode, of which the electric field is orientated normally to the sample surfaces [for determination of $\varepsilon'_{\perp}$—cases in Fig. 3(b)]. The multilayer sample is placed at the resonator floor $(h_4 = 0)$. Resonator R2 should have a small enough height $H \leq D/2$ or even $\cong D/3$ to remove higher order modes (such as TE modes) from the TM_{010}-mode resonance curve.

The exact dispersion equations of TE and TM modes in the resonance cavities under consideration with three-layer lossless samples can be described in the general case as follows.

1) *Dispersion equations for* TE_{nmp} *modes* ($n = 0, 1, 2, \ldots$, $m = 1, 2, 3, \ldots, p = 1, 2, 3, \ldots$) (see Fig. 2) [see Fig. 3(a)]

$$
\begin{aligned}
&\beta_1 \tan\beta_1 h_1 \left(\frac{\tan\beta_2 h_2}{\beta_2} + \frac{\tan\beta_4 h_4}{\beta_4}\right)\left(\frac{\tan\beta_3 h_3}{\beta_3} + \frac{\tan\beta_5 h_5}{\beta_5}\right)\\
&\quad + \frac{\beta_2}{\beta_4}\tan\beta_2 h_2 . \tan\beta_4 h_4\\
&\quad \times \left(\frac{\tan\beta_1 h_1}{\beta_1} + \frac{\tan\beta_3 h_3}{\beta_3} + \frac{\tan\beta_5 h_5}{\beta_5}\right)\\
&\quad + \frac{\beta_3}{\beta_5}\tan\beta_3 h_3 . \tan\beta_5 h_5\\
&\quad \times \left(\frac{\tan\beta_1 h_1}{\beta_1} + \frac{\tan\beta_2 h_2}{\beta_2} + \frac{\tan\beta_4 h_4}{\beta_4}\right)\\
&\quad - \left(\sum_{i=1}^{5}\frac{\tan\beta_i h_i}{\beta_i} + \frac{\beta_2\beta_3}{\beta_1\beta_4\beta_5}\prod_{i=1}^{5}\tan\beta_i h_i\right) = 0. \qquad (1)
\end{aligned}
$$

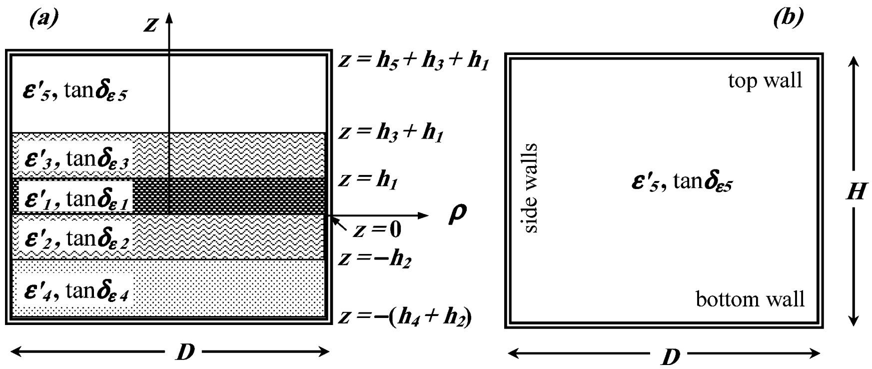

Fig. 4. Resonance cavity filled with lossy materials: (a) with three-layer sample and (b) without sample; empty (or foam-filled) cavity.

2) *Dispersion equations for* TM_{nmp} *modes* ($n = 0, 1, 2, \ldots$, $m = 1, 2, 3, \ldots$, $p = 0, 1, 2, \ldots$) (see Fig. 2) [see $h_4 \equiv 0$; Fig. 3(b)]

$$\left(\frac{\beta_1}{\varepsilon_1}\tan\beta_1 h_1 + \frac{\beta_2}{\varepsilon_2}\tan\beta_2 h_2\right) \times \left(1 - \frac{\beta_5\varepsilon_3}{\beta_3\varepsilon_5}\tan\beta_3 h_3.\tan\beta_5 h_5\right) + \left(\frac{\beta_3}{\varepsilon_3}\tan\beta_3 h_3 + \frac{\beta_5}{\varepsilon_5}\tan\beta_5 h_5\right) \times \left(1 - \frac{\beta_2\varepsilon_1}{\beta_1\varepsilon_2}\tan\beta_1 h_1.\tan\beta_2 h_2\right) = 0. \tag{2}$$

These dispersion equations were obtained using known analytical procedures for satisfying the boundary conditions at the perfect cavity walls and between the lossless layers [22]. In the case of a two- and one-layer sample, they could be obtained from (1) and (2) when $h_3 = 0$ or $h_3 = h_2 = 0$.

The propagation constants β_i ($i = 1, 2, 3, 4, 5$) in (1) and (2) are expressed for the different layers as $\beta_i^2 = (2\pi/\lambda_0)^2\varepsilon_i - (\chi_{nm})^2_{\mathrm{TE,TM}}/R^2$, where $\lambda_0 = c/f_{\mathrm{res}}$, $R = D/2$, (f_{res}—resonance frequency of a given mode excited in the cavity, λ_0—free-space wavelength). In the considered resonators $(\chi_{0m})_{\mathrm{TE}} = \nu'_{0m} = 3.8317, 7.1556, 10.1735\ldots$—for TE_{011}, TE_{021}, and TE_{031} modes and $(\chi_{0m})_{\mathrm{TM}} = \nu_{0m} = 2.4048, 5.5201, 8.6537\ldots$—for TM_{010}, TM_{020}, and TM_{030} modes ($\nu_0; \nu'_0$ are the zeroes of a first-kind Bessel function $J_0(x)$ and its derivative $J'_0(x)$ according to the argument). The dielectric constants ε_i in all layers ($i = 1, 2, 3, 4, 5$) represent either the real part of longitudinal values $\varepsilon'_{||i}$ (for TE_{0mp} modes) or the real part of transversal values $\varepsilon'_{\perp i}$ (for TM_{0m0} modes). It is important to note that the type of tangent functions in the expressions (1.1–3) and (2.1–3) depend on β_i^2 values. If $\beta_i^2 > 0$, these functions are the ordinary oscillating tangents $\tan(\beta_i\, h_i)$, but if $\beta_i^2 < 0$ (i.e., $\beta_i \to j\alpha_i$), they convert into the hyperbolical tangents $\tan(\beta_i\, h_i) \to j\tanh(\alpha_i\, h_i)$. The parameters α_i are the corresponding dissipation constants in different media. However, the dispersion equations have real variables in all cases.

A FORTRAN-code software MLAYER.EXE has been developed to solve the corresponding dispersion equations. Its first option is the determination of a full-mode spectrum in the cavity with multilayer samples (simplifying the mode identification during the measurements). In the second option, it allows the determination of unknown constants $\varepsilon'_{||}$ and $\varepsilon'_{\perp}$ of each layer if the resonance frequency f_ε of a given mode is measured and the other layers have known dielectric constants (the last denoted below as an *extraction procedure*). Finally, the software accomplishes an error analysis if all the measuring errors of the geometrical and resonance parameters have been determined preliminarily.

B. Determination of the Dielectric Loss Tangent in Multilayer Samples

The determination of the dielectric loss tangent (values $\tan\delta_{\varepsilon||}$ and $\tan\delta_{\varepsilon\perp}$) in one unknown layer of a multilayer sample is a more complicated problem as compared to the determination of the corresponding real part of the dielectric constant $\varepsilon'_{||}$ and $\varepsilon'_{\perp}$. Extra parameters have to be measured (in addition to f_ε): $Q_{0\varepsilon}$—unloaded quality (Q) factor of the chosen mode in the cavity with the sample and surface resistance R_S of the cavity walls. If the influence of the dissipation over the resonance frequency could be neglected, independent measurements of the dielectric constant and the dielectric loss tangent are possible for low- and medium-loss materials (like reinforced artificial substrates, sheets, thin films, composite antenna radomes, etc.). This approach is usually based on the representation of the cavity Q factor in terms of integrals of the electric and magnetic fields' squares [23].

Let us consider a three-layer sample in which the middle layer with parameters ε'_1 and $\tan\delta_{\varepsilon 1}$ is unknown (see Fig. 4). This pair of parameters represents either longitudinal values ($\varepsilon'_{1||}$, $\tan\delta_{\varepsilon 1||}$) in resonator R1 ($\mathrm{TE}_{0mp}$ modes) or transversal values ($\varepsilon'_{1\perp}, \tan\delta_{\varepsilon 1\perp}$) in resonator R2 ($\mathrm{TM}_{0m0}$ modes). It is assumed that the dielectric constant ε'_1 of this layer is already determined by solving one-layer equations (1) (for $\varepsilon'_{1||}$) or (2) (for $\varepsilon'_{1\perp}$).

For the determination of the only unknown parameter $\tan\delta_{\varepsilon 1}$, we can express the unloaded Q factor in the resonators with a sample such as

$$Q_{0\varepsilon} = \frac{\omega \sum\limits_{i=1}^{5} W_i}{\left(\sum\limits_{i=1}^{5} P_i + \sum\limits_{i=1}^{5} P_{Wi} + P_{\mathrm{top}} + P_{\mathrm{bottom}}\right)} \tag{3}$$

where W_i are the values of stored energy in all the considered parts of the resonance cavity, P_i are the dissipated powers

TABLE I
LIMITS FOR INTEGRATION IN (6)–(8)

Layer (i)	1	2	3	4	5
z_1	0	$-h_2$	h_1	$-(h_4+h_2)$	h_3+h_1
z_2	h_1	0	h_3+h_1	$-h_2$	$h_5+h_3+h_1$

within these parts due to the dielectric losses, P_{Wi} are the powers dissipated in the cavity sidewalls in corresponding regions, $P_{\mathrm{top.bottom}}$ are the powers dissipated in both cavity flanges, and $\omega = 2\pi f_\varepsilon$. All these quantities are time averaged. W_4, P_4, and $P_{W4} = 0$ in resonator R2. The unknown parameter $\tan\delta_{\varepsilon 1}$ occurs only in the expression for the dissipated power $P_1 = \tan\delta_{\varepsilon 1}\omega W_1$. Therefore, we get

$$\tan\delta_{\varepsilon 1} = \frac{P_1}{\omega W_1} \tag{4}$$

where

$$P_1 = \frac{\omega \sum_{i=1}^{5} W_i}{Q_{0\varepsilon}} - \left(\sum_{i=2}^{5} P_i + \sum_{i=1}^{5} P_{Wi} + P_{\mathrm{top}} + P_{\mathrm{bottom}}\right). \tag{5}$$

We can separately express the energy and power terms in (5) for resonators R1 and R2 similar to the calculation procedure described in [23]. The stored-energy and dissipated-power terms are defined as

$$W_i = \frac{\varepsilon_i'\varepsilon_0}{2}\int_{z=z_1}^{z_2}\int_{\varphi=0}^{2\pi}\int_{\rho=0}^{R}\left|E_\Sigma^{(i)}\right|^2\rho d\rho d\varphi dz \tag{6}$$

$$P_i = \tan\delta_{\varepsilon i}\omega W_i \tag{7}$$

$$P_{Wi} = \frac{R_s}{2}\int_{z=z_1}^{z_2}\int_{\varphi=0}^{2\pi}\left|H_t^{(i)}\right|^2\rho d\varphi dz|_{\rho=R} \tag{8}$$

$$P_{\mathrm{bottom}} = \frac{R_s}{2}\int_{\rho=0}^{R}\int_{\varphi=0}^{2\pi}\left|H_t^{(4)}\right|^2\rho d\rho d\varphi|_{z=-(h_4+h_2)} \tag{9.1}$$

$$P_{\mathrm{top}} = \frac{R_s}{2}\int_{\rho=0}^{R}\int_{\varphi=0}^{2\pi}\left|H_t^{(5)}\right|^2\rho d\rho d\varphi|_{z=h_5+h_3+h_1} \tag{9.2}$$

where $|E_\Sigma^{(i)}|^2$ are the squares of the total electric field in separate resonator volumes (superscript $^{(i)}$ denotes the different layers in Fig. 4, values z_1 and z_2 for each integral in (6)–(8) are given in Table I), $|H_t^{(i)}|^2$ are the squares of the tangential magnetic-field components to the resonator wall surfaces, and R_S is the known surface impedance on these walls.

1) Case: Resonator **R1**, TE_{0mp} *Modes:* The azimuthally symmetrical TE_{0mp} modes have three field components only—E_φ, H_ρ, and H_z, of which the spatial dependencies in the corresponding areas ($i = 1, 2, 3, 4, 5$) are given as follows (the time factor $\exp(j\omega\, t)$ is not included):

$$H_z^{(i)} = J_0(\tau_{0m}\rho)[A_i\sin\beta_i z + B_i\cos\beta_i z] \tag{10.1}$$

$$H_\rho^{(i)} = \frac{\beta_i}{\tau_{0m}}J_0'(\tau_{0m}\rho)[A_i\cos\beta_i z - B_i\sin\beta_i z] \tag{10.2}$$

$$E_\varphi^{(i)} = j\frac{\omega\mu_0}{\tau_{0m}}J_0'(\tau_{0m}\rho)[A_i\sin\beta_i z + B_i\cos\beta_i z] \tag{10.3}$$

where $\tau_{0m} = (\chi_{0m})_{\mathrm{TE}}/R$. Now we have to substitute the field dependencies (10.1)–(10.3) into (6)–(9) taking into account that $|E_\Sigma^{(i)}|^2 = |E_\varphi^{(i)}|^2$ in all regions, while the corresponding tangential magnetic fields are $H_t^{(i)} = H_z^{(i)}$ at the side resonator walls and $H_t^{(4,5)} = H_\rho^{(4,5)}$ at the top and bottom flanges. We obtain for the energy-stored and dissipated-power terms in (5), (11)–(16) with superscript $^{\mathrm{TE}0m}$ given below. The known properties of the trigonometrical and first-kind Bessel functions and the equality $J_0'(\tau_{0m}R) = 0$ for TE_{0mp} modes are used for the following analytical calculations:

$$W_i^{\mathrm{TE}_{0m}} = V_i^{\mathrm{TE}_{0m}} J_0^2(\tau_{0m}R)F_i^{\mathrm{TE}_{0m}} \tag{11.1}$$

$$P_{Wi}^{\mathrm{TE}_{0m}} = S_i^{\mathrm{TE}_{0m}} J_0^2(\tau_{0m}R)F_i^{\mathrm{TE}_{0m}} \tag{11.2}$$

$$P_{\mathrm{bottom}}^{\mathrm{TE}_{0m}} = \frac{T_4^{\mathrm{TE}_{0m}} J_0^2(\tau_{0m}R)A_4^2}{\cos^2\beta_4(h_4+h_2)} \tag{12.1}$$

$$P_{\mathrm{top}}^{\mathrm{TE}_{0m}} = \frac{T_5^{\mathrm{TE}_{0m}} J_0^2(\tau_{0m}R)A_5^2}{\cos^2\beta_5(h_5+h_3+h_1)} \tag{12.2}$$

with terms after the integration expressed as

$$F_i^{\mathrm{TE}_{0m}} = A_i^2X_i + B_i^2Y_i + 2A_iB_iZ_i, \qquad i=1,2 \tag{13.1,2}$$

$$F_3^{\mathrm{TE}_{0m}} = A_3^2 + B_3^2 + \left(A_3^2 - B_3^2\right)Y_3 + 2A_3B_3Z_3 \tag{13.3}$$

$$F_4^{\mathrm{TE}_{0m}} = \frac{A_4^2X_4}{\cos^2\beta_4(h_4+h_2)} \tag{13.4}$$

$$F_5^{\mathrm{TE}_{0m}} = \frac{A_5^2X_5}{\cos^2\beta_5(h_5+h_3+h_1)}. \tag{13.5}$$

The following denotations are used above:

$$V_i^{\mathrm{TE}_{0m}} = \frac{\varepsilon_i'\left(\frac{\omega}{c}\right)^2\mu_0\pi R^2h_i}{4\tau_{0m}^2}, \qquad i = 1,2,3,4,5 \tag{14.1}$$

$$S_i^{\mathrm{TE}_{0m}} = \frac{R_S^{\mathrm{TE}_{0m}}\pi Rh_i}{2}, \qquad i = 1,2,3,4,5 \tag{14.2}$$

$$T_i^{\mathrm{TE}_{0m}} = \frac{R_S^{\mathrm{TE}_{0m}}\pi R^2\beta_i^2}{2\tau_{0m}^2}, \qquad i = 4,5 \tag{14.3}$$

$$X_i = 1 - \frac{\sin(2\beta_ih_i)}{2\beta_ih_i}, \qquad i = 1,2,4,5 \tag{15.1}$$

$$Y_i = 1 + \frac{\sin(2\beta_ih_i)}{2\beta_ih_i} \tag{15.2}$$

$$Z_i = \frac{1-\cos(2\beta_ih_i)}{2\beta_ih_i} \tag{15.3}$$

$$Y_3 = \sin\beta_3h_3 \times \frac{\cos\beta_3(h_3+2h_1)}{\beta_3h_3} \tag{16.1}$$

$$Z_3 = \sin\beta_3h_3 \times \frac{\sin\beta_3(h_3+2h_1)}{\beta_3h_3}. \tag{16.2}$$

The unknown field constants A_i and B_i are connected with the following relations due to the boundary conditions—continuity of the tangential electric and magnetic field components at the surfaces between the cavity parts:

$$\begin{aligned}
A_1 &= \frac{\Delta_{A1}}{\Delta_{\mathrm{TE}}}\\
B_1 &= \frac{\Delta_{B1}}{\Delta_{\mathrm{TE}}}\\
A_4 &= \frac{\Delta_{A4}}{\Delta_{\mathrm{TE}}}\\
A_2 &= \left(\frac{\beta_1}{\beta_3}\right) A_1\\
B_2 &= B_1\\
A_3 &= \xi_4 (A_1 K_1 + A_2 K_2)\\
B_3 &= \xi_4 (A_1 K_3 + A_2 K_4)\\
B_4 &= A_4 \tan\beta_4 (h_4 + h_2);\\
B_5 &= -A_5 \tan\beta_5 (h_5 + h_3 + h_1)
\end{aligned} \tag{17.1}$$

where

$$\begin{aligned}
\Delta_{A1} &= \beta_5 A_5 \xi_1 \Delta_A\\
\Delta_{B1} &= -\beta_5 A_5 \xi_1 \Delta_B\\
\Delta_{A4} &= -\beta_1 \beta_5 A_5 \xi_1\\
\Delta_{\mathrm{TE}} &= \Theta_1 \Delta_A - \Theta_2 \Delta_B\\
\Delta_A &= -\beta_4 \xi_2 L_1\\
\Delta_B &= \beta_4 \xi_2 L_2\\
\Theta_1 &= \beta_3 \xi_3 (K_2 - K_4)\\
\Theta_2 &= \beta_3 \xi_3 (K_1 - K_3)
\end{aligned} \tag{17.2}$$

and

$$\begin{aligned}
\xi_1 &= \frac{\cos\beta_5 h_5}{\cos\beta_5 (h_5 + h_3 + h_1)}\\
\xi_2 &= \frac{\cos\beta_2 h_2 \times \cos\beta_4 h_4}{\cos\beta_4 (h_4 + h_2)}\\
\xi_3 &= \xi_4 \cos\beta_3 (h_3 + h_1)\\
\xi_4 &= \cos\beta_3 h_1 \times \cos\beta_1 h_1\\
K_1 &= \frac{\beta_1}{\beta_3} + \tan\beta_3 h_1 \times \tan\beta_1 h_1\\
K_2 &= \tan\beta_3 h_1 - \left(\frac{\beta_1}{\beta_3}\right) \tan\beta_1 h_1\\
K_3 &= \tan\beta_1 h_1 - \left(\frac{\beta_1}{\beta_3}\right) \tan\beta_3 h_1\\
K_4 &= 1 + \left(\frac{\beta_1}{\beta_3}\right) \tan\beta_3 h_1 \times \tan\beta_1 h_1\\
L_1 &= 1 - \left(\frac{\beta_2}{\beta_4}\right) \tan\beta_4 h_4 \times \tan\beta_2 h_2\\
L_2 &= \left(\frac{\beta_1}{\beta_2}\right) \tan\beta_2 h_2 + \left(\frac{\beta_1}{\beta_4}\right) \tan\beta_4 h_4.
\end{aligned} \tag{17.3}$$

Finally, we can calculate the necessary value of the longitudinal dielectric loss tangent $\tan\delta_{\varepsilon 1\|}$ of the middle layer substituting the energy and power terms from (11)–(14) into (4) and (5). The only unknown parameter is the surface resistance R_S, which could be determined by the resonance parameters of empty resonator R1 (see Section III for details).

2) Case: Resonator $\mathbf{R2}$*,* TM_{0m0} *modes* $(h_4 = 0)$*:* These modes also have three field components E_ρ, E_z, and H_φ; their spatial dependencies are presented by (18.1)–(18.3); $i = 1, 2, 3, 5)$

$$E_z^{(i)} = J_0(\theta_{0m}\rho)[C_i \sin\beta_i z + D_i \cos\beta_i z] \tag{18.1}$$

$$E_\rho^{(i)} = \frac{\beta_i}{\theta_{0m}} J_0'(\theta_{0m}\rho)[C_i \cos\beta_i z - D_i \sin\beta_i z] \tag{18.2}$$

$$H_\varphi^{(i)} = -j\frac{\omega\varepsilon_0\varepsilon_i'}{\theta_{0m}} J_0'(\theta_{0m}\rho)[C_i \sin\beta_i z + D_i \cos\beta_i z] \tag{18.3}$$

where $\theta_{0m} = (\chi_{0m})_{\mathrm{TM}}/R$. The unknown constants in this case can be expressed with the following relations:

$$\begin{aligned}
D_2 &= \frac{\Delta_{D2}}{\Delta_{\mathrm{TM}}}\\
C_3 &= \frac{\Delta_{C3}}{\Delta_{\mathrm{TM}}}\\
D_3 &= \frac{\Delta_{D3}}{\Delta_{\mathrm{TM}}}\\
C_4 &= D_4 \equiv 0\\
C_1 &= -\left(\frac{\beta_1}{\beta_3}\right) D_2 \tan\beta_2 h_2\\
D_1 &= \left(\frac{\varepsilon_2}{\varepsilon_1}\right) D_2\\
C_2 &= -D_2 \tan\beta_2 h_2\\
C_5 &= D_5 \tan\beta_5 (h_5 + h_3 + h_1)
\end{aligned} \tag{19.1}$$

where

$$\begin{aligned}
\Delta_{D2} &= \varepsilon_5 \varepsilon_3 \beta_3 \xi_1 D_5\\
\Delta_{C3} &= -\varepsilon_5 \xi_1 \Delta_C D_5\\
\Delta_{D3} &= \varepsilon_5 \xi_1 \Delta_D D_5\\
\Delta_{\mathrm{TM}} &= \Xi_1 \Delta_D - \Xi_2 \Delta_C\\
\Xi_1 &= \varepsilon_3 \cos\beta_3 (h_3 + h_1)\\
\Xi_2 &= \varepsilon_3 \sin\beta_3 (h_3 + h_1)
\end{aligned} \tag{19.2}$$

and

$$\begin{aligned}
\Delta_D &= \varepsilon_1 \varepsilon_3 \xi_4 \left[\left(\frac{\beta_1}{\varepsilon_1}\right) N_1 \tan\beta_3 h_1 + \left(\frac{\beta_3}{\varepsilon_3}\right) N_2\right]\\
\Delta_C &= \varepsilon_1 \varepsilon_3 \xi_4 \left[\left(\frac{\beta_1}{\varepsilon_1}\right) N_1 - \left(\frac{\beta_3}{\varepsilon_3}\right) N_2 \tan\beta_3 h_1\right]\\
N_1 &= \left(\frac{\beta_2}{\beta_1}\right) \tan\beta_2 h_2 + \left(\frac{\varepsilon_2}{\varepsilon_1}\right) \tan\beta_1 h_1\\
N_2 &= \left(\frac{\varepsilon_2}{\varepsilon_1}\right) - \left(\frac{\beta_2}{\beta_1}\right) \tan\beta_2 h_2 \times \tan\beta_1 h_1.
\end{aligned} \tag{19.3}$$

In this case, we can use another expression for the energy and power terms (with superscript $^{\mathrm{TM}0m}$) in (5). The square of the total electric field is now $|E^{(i)}|^2 = |E_\rho^{(i)}|^2 + |E_z^{(i)}|^2$, while the tangential magnetic field is $H_t^{(i)} = H_\varphi^{(i)}$ everywhere. The equality $J_0(\theta_{0m}R) = 0$ for the TM_{0m0} modes is valid. After new substitutions of the field dependencies from (18.1)–(18.3) into (6)–(9) ($h_4 = 0$), we get

$$W_i^{\mathrm{TM}_{0m}} = V_i^{\mathrm{TE}_{0m}} J_1^2(\theta_{0m}R) F_i^{\mathrm{TM}_{0m}} \tag{20.1}$$
$$P_{Wi}^{\mathrm{TM}_{0m}} = S_i^{\mathrm{TM}_{0m}} J_1^2(\theta_{0m}R) F_i^{\mathrm{TM}_{0m}} \tag{20.2}$$
$$P_{\mathrm{bottom}}^{\mathrm{TM}_{0m}} = \frac{T_2^{\mathrm{TM}_{0m}} J_1^2(\theta_{0m}R) D_2^2}{\cos^2 \beta_2 h_2} \tag{21.1}$$
$$P_{\mathrm{top}}^{\mathrm{TM}_{0m}} = \frac{T_5^{\mathrm{TM}_{0m}} J_1^2(\theta_{0m}R) D_5^2}{\cos^2 \beta_5 (h_5 + h_3 + h_1)} \tag{21.2}$$

with corresponding terms after the integration expressed as

$$F_1^{\mathrm{TM}_{0m}} = C_1^2 X_1 + D_1^2 Y_1 + 2C_1 D_1 Z_1 \tag{22.1}$$
$$F_2^{\mathrm{TM}_{0m}} = \frac{D_2^2 X_2}{\cos^2 \beta_2 h_2} \tag{22.2}$$
$$F_3^{\mathrm{TM}_{0m}} = C_3^2 + D_3^2 - \left(C_3^2 - D_3^2\right) Y_3 + 2C_3 D_3 Z_3 \tag{22.3}$$
$$F_5^{\mathrm{TM}_{0m}} = \frac{D_5^2 X_5}{\cos^2 \beta_5 (h_5 + h_3 + h_1)} \tag{22.4}$$

where

$$V_i^{\mathrm{TM}_{0m}} = \frac{\varepsilon_i'^2 \varepsilon_0 \left(\frac{\omega}{c}\right)^2 \pi R^2 h_k}{4\theta_{0m}}, \qquad i = 1, 2, 3, 5 \tag{23.1}$$
$$S_i^{\mathrm{TM}_{0m}} = \frac{R_S^{\mathrm{TM}_{0m}} \varepsilon_i'^2 \varepsilon_0 \left(\frac{\omega}{c}\right)^2 \pi R h_i}{2\mu_0 \theta_{0m}^2} \tag{23.2}$$
$$T_i^{\mathrm{TM}_{0m}} = \frac{R_S^{\mathrm{TM}_{0m}} \varepsilon_i'^2 \varepsilon_0 \left(\frac{\omega}{c}\right)^2 \pi R^2}{2\mu_0 \theta_{0m}^2}, \qquad i = 2, 5. \tag{23.3}$$

The value of the transversal dielectric loss tangent $\tan \delta_{\varepsilon 1 \perp}$ of the middle layer could be computed from (4) and (5) by the substitution of the energy and power terms from (20)–(23). In this case, the unknown surface resistance R_S is determined from measurement results of the empty resonator R2.

3) Determination of the Surface Resistance R_S: The preliminary determination of the surface resistance values in both resonance cavities is absolutely necessary for the measurement accuracy improvement. There are two possibilities to obtain these values. The simplest way is to use the known formula (see [24, pp. 25-26])

$$R_S = \sqrt{\frac{\pi f_\varepsilon \mu_W \mu_0}{\sigma_W}} \tag{24}$$

where σ_W is the catalog value of the wall conductivity and μ_W is the relative wall permeability.

A more accurate way is the determination of the actual value of the surface resistance, as in [25] and [26], for the measurement of the dielectric rod samples or in [27] for the characterization of HTS films. In our case, we use the measurement results, namely, the resonance frequency $\omega_0 = 2\pi f_0$ and the unloaded Q factor Q_0 of the empty (or foam filled) resonators in order to calculate the actual value of R_S in each resonator (we use one average value for all resonator walls)

$$R_{S0}^{\mathrm{TE}_{0m}} = \frac{\varepsilon_5' \left(\frac{\omega_0}{c}\right)^2 \omega_0 \mu_0 H}{4\tau_{0m}^2} \left(\frac{1}{Q_0^{\mathrm{TE}_{0m}}} - \tan \delta_{\varepsilon 5}\right) \times \left(\frac{H}{2R} + \frac{\beta_5^2}{\tau_{0m}^2}\right)^{-1} \tag{25}$$

for resonator R1 and

$$R_{S0}^{\mathrm{TM}_{0m}} = \frac{H\theta_{0m}^2}{2\omega_0 \varepsilon_5' \varepsilon_0 \left(1 + \frac{H}{R}\right)} \left(\frac{1}{Q_0^{\mathrm{TM}_{0m}}} - \tan \delta_{\varepsilon 5}\right) \tag{26}$$

for resonator R2. Using the computed values for R_S (at the frequency f_0), we can get a pair of equivalent values $\sigma_{W\mathrm{eq}}$ of the wall conductivity for each measurement resonator from

$$\sigma_{W\mathrm{eq}} = \frac{\pi f_0 \mu_W \mu_0}{R_S^2}. \tag{27}$$

Both equivalent values of $\sigma_{W\mathrm{eq}}$ should be used in (24) in order to recalculate the surface resistances $(R_S)^{\mathrm{TE,\,TM}}$ at the resonance frequency f_ε of the cavities with the sample. Then (14.2), (14.3), (23.2), and (23.3) with the actual values $\sigma_{W\mathrm{eq}}$ can be used for the calculation of the dielectric loss tangent in each direction.

III. Measurement Sensitivity and Errors

A. Measuring Resonance Cavities

There are two possibilities to realize the proposed two-resonator method, which are: 1) both the measuring resonators have equal diameters $D^{R1} = D^{R2}$ and the measurement of $\varepsilon'_{\parallel}$ and $\varepsilon'_{\perp}$ corresponds to different resonance frequencies denoted as $f_\varepsilon^{\mathrm{TE011}} > f_\varepsilon^{\mathrm{TM010}}$ (this case is more suitable for materials with a relatively weak frequency dependence on the dielectric constant and loss tangent) and 2) the resonators have diameters $D^{R1} > D^{R2}$, for which the values of $\varepsilon'_{\parallel}$ and $\varepsilon'_{\perp}$ are determined at relatively close frequencies $f_\varepsilon^{\mathrm{TE011}} \sim f_\varepsilon^{\mathrm{TM010}}$. One nonmetallized sample is needed for the first case (the variations in the parameters from sample to sample could be avoided), while two separate samples with differing diameters have to be prepared for the second case. In this paper, we present examples for the both cases. The resonator dimensions are designed to be $D^{R1} = 30.00$ mm, $H^{R1} = 29.82$ mm (for R1), and $D^{R2} = 30.00$ mm, $H^{R2} = 12.12$ mm (for $R2'$), or $D^{R2} = 18.1$ mm, $H^{R2} = 12.09$ mm (for R2) [see Fig. 5(a) and (b)]. The corresponding measured resonance frequencies and unloaded Q factors of the empty resonators are $f_0^{\mathrm{TE011}} = 13.1519$ GHz, $Q_0^{\mathrm{TE011}} = 14\,470$ in R1 and $f_0^{\mathrm{TM010}} = 7.6385$ GHz, $Q_0^{\mathrm{TM010}} = 3850$ in $R2'$ (or $f_0^{\mathrm{TM010}} = 12.6404$ GHz, $Q_0^{\mathrm{TM010}} = 3552$ in R2). All these parameters are obtained with "daily" variations of $\pm 0.01\%$ in the resonance frequency and $\pm 1.5\%$ in the Q factor (mainly due

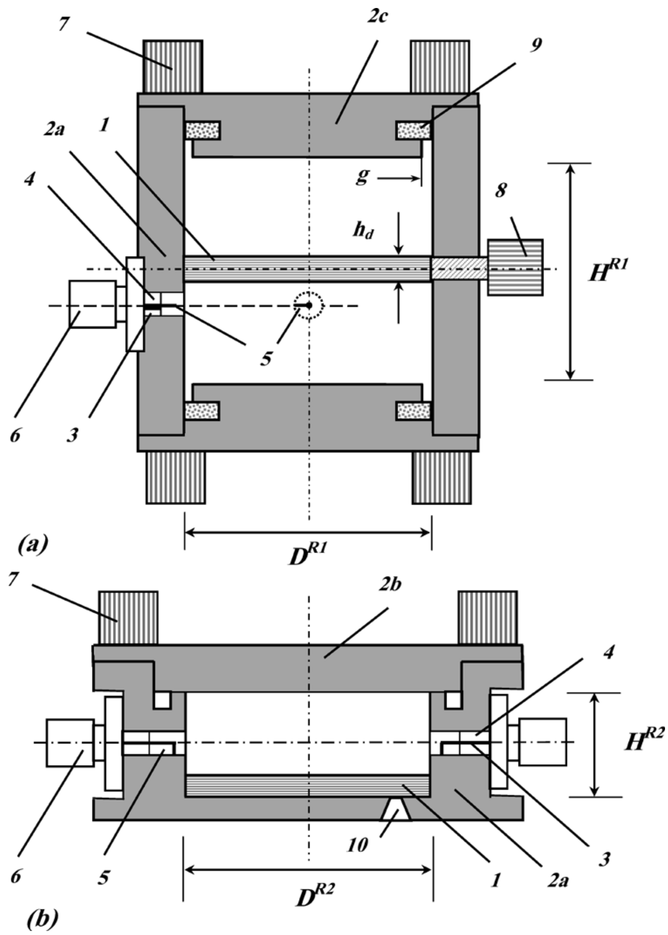

Fig. 5. Practical realization of both measurement cavities. (a) **R1**. (b) **R2**. Denotations: (1) multilayer sample, (2a) gold-plated resonator body, (2b) flange with improved dc contact, (2c) contactless flanges with gap $g \sim 0.35$ mm, (3) coaxial section 2.2/0.8 mm, (4) Teflon bush, (5) exciting semiloops, (6) SMA connectors, (7) mounting screws, (8) screw holder for the sample, (9) 1-mm-thick rubber absorber (Eccosorb BSR-2), (10) hole for pulling the sample trough the cavity.

to room-temperature changes, cavity cleanness, and influence of tuning elements).

The cross-sectional view of measuring resonators R1 and R2 shows that they have special features concerning the working conditions; nevertheless, they are both cylindrical resonance cavities. Resonator R1 [see Fig. 5(a)] has two movable "contactless" flanges with absorbing rings in order to suppress the unwanted TM modes here (compression better than -60 dB). Two subminiature A (SMA) connectors at an azimuthal angle of 90° slightly below the middle of the resonator with exciting semiloops with axis parallel to the resonator axis are arranged on the cavity sidewalls. Thus, the excited symmetrical $\mathrm{TE}_{011}, \mathrm{TE}_{021}, \mathrm{TE}_{013}, \ldots$ modes are suitable at these conditions for measurement purposes of longitudinal dielectric parameters, while the $\mathrm{TE}_{012}, \mathrm{TE}_{014}, \ldots$ modes are not. A limitation is observed with excitations of parasitic $\mathrm{TE}_{112}, \mathrm{TE}_{122}, \ldots$ modes, which are not sensitive to the dielectric sample placed in the resonator half-height. For example, coincidence between the resonance curves of the TE_{011} and TE_{112} modes restricts the dielectric parameters' measurement at this frequency. Another problem is the sample positioning in R1. Two thin screw holders are used to laterally press the sample, but a pair of low-loss foamed supports is also applicable.

Resonator R2 [see Fig. 5(b)] has one movable flange with an improved dc contact and two SMA connectors at 180° in the resonator middle with exciting semiloops axis perpendicularly to the resonator axis. Only a resonator height reduction $(H < R)$ is used here to ensure single-mode regime measurements of the transversal dielectric parameters using the lowest order TM_{010} mode. Measurements with TM_{020} and TM_{030} modes are also possible, but the near presence of parasitic high-order modes makes the mode identification more difficult.

B. Measurement Errors

Here we present a short error analysis of the measuring errors based on software calculations with the program MLAYER (see Section II-A) without writing of direct formulas. The analysis is simple: we vary the values of one parameter (e.g., sample height) keeping the values of all other parameters and calculate the particular relative variation of the permittivity and loss tangent values. Finally, we estimate the needed relative error as a sum of these particular relative variations.

It is a known fact that the contributions of the separate parameter variations are very different. The main sources of errors in the proposed two-resonator method are due to uncertainties for the determination of the parameters D, H, h_i, and f_ε and the sample positioning in the resonance cavities. Measurements of the resonance frequencies are usually precise; therefore, the measuring errors mainly depend on the geometrical parameters. However, a detectable difference is usually observed between the measured $(f_0)_{\mathrm{meas}}$ and calculated $(f_0)_{\mathrm{calc}}$ resonance frequencies in both empty resonators due to a variety of reasons: coupling effects of connectors, influence of supporting screws, resonator elliptical eccentricity, contactless flange influence in R1, holes influence in R2, etc. A suitable solution of this problem is to introduce an *equivalent cavity diameter* $(D_{\mathrm{eq}})_{\mathrm{TE,\ TM}}$ for each of the considered modes in order to ensure an exact equality $(f_0)_{\mathrm{meas\ TE,TM}} \equiv (f_0)_{\mathrm{calc\ TE,TM}}$ in both empty resonators for each mode. We obtained the following equivalent diameters: $(D_{\mathrm{eq}})_{\mathrm{TE011}} = 30.086$ mm (0.29% increase) and $(D_{\mathrm{eq}})_{\mathrm{TM010}} = 30.045$ mm (0.15% increase in $R2'$) or $(D_{\mathrm{eq}})_{\mathrm{TM010}} = 18.155$ mm (0.30% increase in $R2'$). Thus, the use of D_{eq} instead of D allows a minimization of uncertainties due to the resonator dimensions D and H. Therefore, the errors for the measurement of $\varepsilon'_{||}$ and $\varepsilon_\perp$ values mainly depend on relative errors of the sample height determination $\Delta h_1/h_1$ (Fig. 6) and weakly on the sample positioning $\Delta h_5/h_5$ in the cavity middle.

A similar problem appears for the unloaded Q factors of the empty resonators; namely, the measured value is smaller than the theoretical one. For example, the theoretical Q factor for the TE_{011} mode in R1 is $Q_{0\mathrm{th}} = 22\,125$ for gold conductivity $\sigma_{\mathrm{Au}} = 4.1 \times 10^7$ S/m and theoretical surface resistance $R_{S\mathrm{th}} = 35.3$ mΩ (at $f_0 = 13.1519$ GHz). The measured value is $Q_0 = 14\,470$, which corresponds to a measured surface resistance $R_{S0} = 53.9$ mΩ, obtained from (30) and *equivalent conductivity* $\sigma_{W\mathrm{eq}} = 1.8 \times 10^7$ S/m calculated from (32). The corresponding theoretical values for the TM_{010} mode

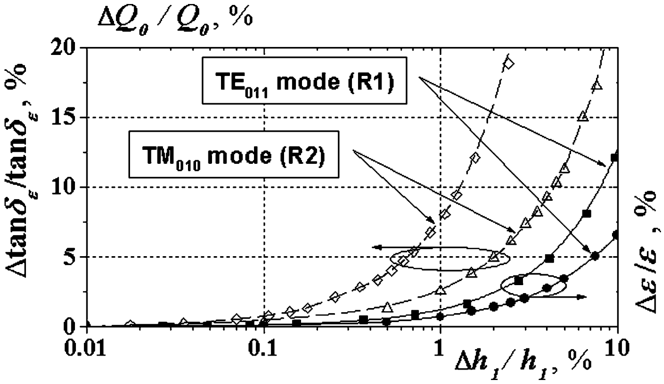

Fig. 6. Measurement relative errors in resonators R1 and R2.

TABLE II
MEASURED DIELECTRIC PARAMETERS OF PURE ISOTROPIC SAMPLES WITH THICKNESS OF 1.00 mm (TRANSPARENT POLYCARBONAT)

D_{eq}, mm (R1)	$\varepsilon'_{\parallel}$ f_ε, GHz	D_{eq}, mm (R2)	$\varepsilon'_{\perp}$ f_ε, GHz	D_{eq}, mm (R2)	$\varepsilon'_{\perp}$ f_ε, GHz
30.087	2.767 12.3221	30.047	2.726 7.4218	18.156	2.768 12.2325
σ_{eq}, S/m (R1)	$\tan\delta_{\varepsilon\parallel}$ $Q_{0\varepsilon}$	σ_{eq}, S/m (R2)	$\tan\delta_{\varepsilon\perp}$ Q_0	σ_{eq}, S/m (R2)	$\tan\delta_{\varepsilon\perp}$ Q_0
1.7×10^7	0.00564 775	1.1×10^7	0.00536 2154	0.9×10^7	0.00563 1768
D, mm; σ_{Au}, S/m	$\varepsilon'_{\parallel}$, $\tan\delta_{\varepsilon\parallel}$	D, mm; σ_{Au}, S/m	$\varepsilon'_{\perp}$, $\tan\delta_{\varepsilon\perp}$	D, mm; σ_{Au}, S/m	$\varepsilon'_{\perp}$, $\tan\delta_{\varepsilon\perp}$
30.00 4.1×10^7	2.830 0.00559	30.00 4.1×10^7	2.973 0.00960	18.10 4.1×10^7	3.153 0.00990

in $R2'$ are $Q_{0\text{th}} = 7482$ and $R_{S\text{th}} = 27.0$ mΩ (at $f_0 = 7.6385$ GHz), while the measured values are $Q_0 = 3850$ and $R_{S0} = 52.5$ mΩ, obtained by (31) and an *equivalent conductivity* $\sigma_{W\text{eq}} = 1.1 \times 10^7$ S/m (for R2: $Q_0 = 3559$, $R_{S0} = 72.3$ mΩ, $\sigma_{W\text{eq}} = 0.94 \times 10^7$ S/m). These results unambiguously show that the determination of the equivalent wall conductivity for each working mode is absolutely necessary for a decrease of the relative errors of measurements of the loss tangent.

Taking into account the above-discussed issues, the measuring errors in the presented method can be estimated as follows: <1.0%–1.5% for $\varepsilon'_{\parallel}$ and <5% for $\varepsilon'_{\perp}$ for a reference sample like RO3203 with a thickness of 0.254 mm measured with errors $\Delta h_1/h_1 < 2\%$ (that is the main source of measurement errors for the permittivity, Fig. 6). Besides, even the positioning uncertainty $\Delta h_5/h_5$ reaches a value of 10% (i.e., even $\Delta h_5 \sim \pm 1.5$ mm) for the sample positioning in R1, the relative measurement error of $\varepsilon'_{\parallel}$ does not exceed the value of 2.5%. The measuring errors for the determination of the dielectric loss tangent are estimated as 5%–7% for $\tan\delta_{\varepsilon\parallel}$, but up to 25% for $\tan\delta_{\varepsilon\perp}$, when the measuring error for the unloaded Q factor is 5% (that is the main additional source for the loss-tangent errors; the other one is the dielectric constant error).

C. Measurement Sensitivity

A real problem of the proposed method for the determination of the dielectric anisotropy ΔA_ε is the measurement sensitivity of the TM_{010} mode in resonator R2 (for $\varepsilon_\perp$), which is noticeably smaller compared to the sensitivity of the TE_{011} mode in R1 (for $\varepsilon'_{\parallel}$). We illustrate this effect in [8], where the curves of the resonance frequency shift versus the dielectric constant have been presented for one-layer samples with height h_1 from 0.125 to 1.5 mm. The shift $\Delta f/\Delta\varepsilon$ in R1 for a sample with $h_1 = 0.5$ mm is a decrease of 480 MHz for the doubling of $\varepsilon'_{\parallel}$ (from 2 to 4), while the corresponding shift in R2 is only a decrease of 42.9 MHz for the doubling of $\varepsilon_\perp$. Also, the Q factor of the TM_{010} mode in R2 is smaller compared to the Q factor of the TE_{011} mode in R1. This leads to an unequal accuracy for the determination of the loss tangent anisotropy $\Delta A_{\tan\delta\varepsilon}$.

Thus, the measured anisotropy for the dielectric constant $\Delta A_\varepsilon < 2.5\%$–$3\%$ and for the dielectric loss tangent $\Delta A_{\tan\delta\varepsilon} < 10\%$–$12\%$ could be associated with a *practical isotropy* of the sample ($\varepsilon'_{\parallel} \cong \varepsilon'_{\perp}$; $\tan\delta_{\varepsilon\parallel} \cong \tan\delta_{\varepsilon\perp}$) because these differences fall into the measurement error margins.

A natural test for the proposed two-resonator method is the determination of the dielectric parameters of a clearly expressed isotropic material. We have chosen for this test 1-mm-thick samples from LEXAN D-sheet ($\varepsilon_r \cong 2.8$, $\tan\delta_\varepsilon \cong 0.006$), which is suitable for antenna radomes. The measured results in resonators R1, R2′ ($D = 30.0$ mm) and R2 ($D = 18.1$ mm) are presented in Table II (averaged from five samples). For each resonator, we determine its equivalent diameter $(D_{\text{eq}})_{\text{TE, TM}}$ and its equivalent wall conductivity $(\sigma_{W\text{eq}})_{\text{TE, TM}}$. When we use these equivalent parameters, the measured "anisotropy" ΔA_ε and $\Delta A_{\tan\delta\varepsilon}$ for the isotropic samples is less than 1% for the dielectric constant and less than 5% for the dielectric constant, i.e., the practical isotropy of this material is obvious. Very important is the fact that, if the physical diameters D^{R1} or D^{R2} are used in the calculation instead the equivalent ones, higher values for the dielectric constant will be obtained. For example, the increase is ~2.3% for $\varepsilon'_{\parallel}$ and 13.9% for $\varepsilon'_{\perp}$, while the measuring errors are only 0.6% for $\varepsilon'_{\parallel}$ and 1.1% for $\varepsilon'_{\perp}$ in this case. Another important conclusion is that the utilization of the equivalent conductivity $\sigma_{W\text{eq}}$ has a decisive influence to the measurement accuracy for the determination of the dielectric loss tangent values, especially in R2 resonator. Actually, if we use $\sigma_{\text{Au}} = 4.1 \times 10^7$ S/m (instead of $\sigma_{W\text{eq}}$), we will obtain higher values for the dielectric loss tangent, e.g., up to 76% for $\tan\delta_{\varepsilon\perp}$, while the measuring uncertainties are smaller: ~2.3% for $\tan\delta_{\varepsilon\parallel}$; ~3.6% for $\tan\delta_{\varepsilon\perp}$.

This useful "isotropic-sample" test allows us to conclude that the proposed two-resonator method has the needed ability to detect as the *practical isotropy*, as well as the *possible anisotropy* of a wide class of microwave materials.

IV. Measurement of Dielectric Anisotropy of Multilayer Samples

We have presented in [8] several examples for estimation of the dielectric constant anisotropy in one-, two-, and three-layer samples by the proposed two-resonator method. In the case of

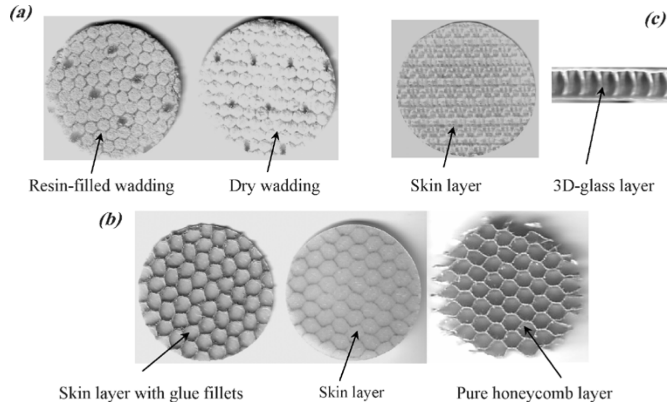

Fig. 7. Illustrative photographs of the measured antenna-radome layers. (a) Example 1. (b) Example 2. (c) Example 3.

TABLE III
EXAMPLE 1: THREE-LAYER ANTENNA RADOME WITH RESIN PENETRATION INTO THE MIDDLE WADDING LAYER

Antenna-radome layers	h_i, mm	$\varepsilon'_{\parallel}$	$\varepsilon'_{\perp}$	$\tan\delta_{\varepsilon\parallel}$	$\tan\delta_{\varepsilon\perp}$
Whole sandwish-type radome: measured parameters: f_ε = 12.1876 GHz; $Q_{0\varepsilon}$ = 304 (TE_{011} mode in R1); f_ε= 11.9801 GHz; $Q_{0\varepsilon}$ = 424 (TM_{010} mode in R2)					
"average" sample	2.17 ± 0.02	1.97 ± 0.02	1.82 ± 0.03	0.0100 ± 0.0005	0.0120 ± 0.0008
Separate layers:					
Dry wadding layer	1.72	1.069	1.058	0.0014	0.0012
Top/bottom E-glass skins	0.20	3.4	2.7	0.018	0.017
Middle layer: resin-filled wadding (2 kg/m^2 resin consumption)					
Extracted values	1.77	1.66	1.70	0.0072	0.011
Measured directly after the skins removing	1.77	1.64 ± 0.04	1.68 ± 0.05	0.0075 ± 0.0005	0.011 ± 0.001

TABLE IV
EXAMPLE 2: THREE-LAYER HONEYCOMB RADOME ([28])—ESTIMATION OF THE GLUE-FILLETS LAYER PARAMETERS

Antenna-radome layers	h_i, mm	$\varepsilon'_{\parallel}$	$\varepsilon'_{\perp}$	$\tan\delta_{\varepsilon\parallel}$	$\tan\delta_{\varepsilon\perp}$
Whole sandwish-type radome: measured parameters: f_ε = 12.1759 GHz; $Q_{0\varepsilon}$ = 289 (TE_{011} mode in R1); f_ε= 12.1595 GHz; $Q_{0\varepsilon}$ = 475 (TM_{010} mode in R2)					
"average" sample	3.16	1.687	1.333	0.0087	0.0071
Separate layers:					
Top/bottom skin layers	0.27	4.00	3.17	0.0177	0.0167
Pure honeycomb layer (measured)	2.62	1.042	1.049	0.0015	0.0038
Honeycomb layer (extracted)	2.62	1.213	1.191	0.0075	0.0061
Skin layer with glue fillets	0.60	2.78	1.83	0.0152	0.0083
Intermediate glue-fillets layer	0.33	1.75	1.53	0.0118	0.0052

TABLE V
EXAMPLE 3: THREE-LAYER 3-D GLASS RADOME [29]

Antenna-radome layers	h_i, mm	$\varepsilon'_{\parallel}$	$\varepsilon'_{\perp}$	$\tan\delta_{\varepsilon\parallel}$	$\tan\delta_{\varepsilon\perp}$
Whole 3D-glass radome: measured parameters: f_ε = 11.7997 GHz; $Q_{0\varepsilon}$ = 242 (TE_{011} mode in R1); f_ε= 11.6669 GHz; $Q_{0\varepsilon}$ = 284 (TM_{010} mode in R2)					
"average" sample	5.25	1.612	1.413	0.0072	0.0067
Separate layers:					
Top/bottom skin layers	0.40	3.37	2.48	0.0151	0.0125
Middle 3D-glass layer	4.45	1.331	1.312	0.0045	0.0060

one-layer materials (e.g., reinforced substrates with several penetrated layers), the obtained data allow us to have another look at the properties of these popular artificial microwave materials—their dielectric anisotropy, information for which is not included into the producer catalogs.

In this paper, we consider three more complicated examples for determination of the layers parameters in three-layer samples used as antenna radomes—see Fig. 7. The analysis of anisotropic radomes shows that the right multilayer radome model strongly depend on the knowledge of the actual dielectric parameters [7].

Our first example illustrates how the two-resonator method allows us to estimate the change of the parameters of the middle layer after the manufacturing. We consider the influence of the resin penetration into a dry wadding layer in three-layer antenna radome—Fig. 7(a). The extraction procedure is simple enough.

1) Determination of $(\varepsilon_\Sigma)_{\parallel,\perp}$ and $(\tan\delta_{\varepsilon\Sigma})_{\parallel,\perp}$ of the whole three-layer sample considered as an "average" one-layer sample.
2) Determination of values $(\varepsilon_{2,3})_{\parallel,\perp}$ and $(\tan\delta_{\varepsilon 2,3})_{\parallel,\perp}$ of the pure top and bottom skin layer (usually available before the radome manufacture).
3) Extraction of $(\varepsilon_1)_{\parallel,\perp}$ and $(\tan\delta_{\varepsilon 1})_{\parallel,\perp}$ of the middle layer.

This procedure is illustrated with the data presented in Table III. An increase of dielectric constants $\varepsilon'_{\parallel}(\varepsilon'_{\perp})$ from 1.069 (1.058) up to 1.66 (1.70) (or 55%–60%) is observed in the middle layer, when the resin penetration is taken into account. The increase for the dielectric loss tangents $\tan\delta_{\varepsilon\parallel}$ $(\tan\delta_{\varepsilon\perp})$ is from 0.0014 (0.0012) up to 0.0086 (0.012) (or 6–10 times).

The next sample considers a contrariwise situation—the resin glue does not penetrate into the middle layer. We measure a commercially available radome [28] with a kevlar-paper honeycomb middle layer (see Table IV) . If both of the epoxy skin layers have been preliminary measured, we can extract the honeycomb-layer parameters using the extraction procedure described in the previous example. These parameters are estimated as worse. However, the visual inspection shows that the resin glue actually forms thin "glue-fillets" layers on the inner surfaces of the both skin layers [see Fig. 7(b)]. The last layers are not able to form independent samples and the estimation of their dielectric parameters is possible only after an extraction from resonance measurements of the cavity with two-layer samples—skin and glue-fillets layer. It turns out that the anisotropy of these layers is strong ($\Delta A_\varepsilon \sim 18\%$; $\Delta A_{\tan\delta\varepsilon} \sim 100\%$), which should be taken into account in the radome design.

The last example considers a type of antenna radome, which, in principle, does not have an independent middle layer after the manufactured three-dimensional (3-D) glass fabrics' radome [29] (see Fig. 7(c) and Table V). The described for the first example extraction procedure allows us to easily obtain the dielectric parameters of this inaccessible for direct measurements middle layer.

The main problem in the considered examples appears when the dielectric parameter values of the separate layers differ considerably or the thickness of the protective layers is very small.

In these cases, the measuring errors increase up to 15% for the dielectric constant and up to 50% for loss tangent determination of the middle low-loss filling medium.

V. CONCLUSIONS

In this paper, we have developed a relatively simple two-resonator method for the determination of the anisotropy ΔA_{ε} of the dielectric constant and the anisotropy $\Delta A_{\tan\delta\varepsilon}$ of the dielectric loss tangent in small disk-shaped multilayer samples. The measuring errors are evaluated as small enough: <1.5% for $\varepsilon'_{||}$, <5% for $\varepsilon_{\perp}$, <5% for $\tan\delta_{\varepsilon||}$, and <15% for $\tan\delta_{\varepsilon\perp}$ in the case of typical substrates like RO3203 (0.254-mm thick). Relatively good accuracy is achieved mainly due to the use of the introduced equivalent parameters—equivalent resonator diameter and equivalent wall conductivity with their "daily" variations. Therefore, one can conclude that the described method has the ability to detect a possible anisotropy of one-, two-, and three-layer materials for many practical cases. The presented examples fully confirm the efficiency of the proposed method to easily test the dielectric anisotropy of multilayer samples as the antenna radomes. The extraction of the unknown dielectric parameters of each layer in multilayer samples is possible if the dielectric parameters of the other layers are known or preliminary measured. The described method is not considered as a reference method for an accurate characterization of materials in special laboratories and equipment; it is proposed for a realization under working conditions. The two-resonator method could be helpful for the RF designer's practice for an easy collection of accurate enough dielectric parameters of a variety of materials to be used in modern simulators to realize more accurate simulations than currently possible in an isotropic approximation.

ACKNOWLEDGMENT

This paper is dedicated to the memory of Bulgarian scientist Prof. S. A. Ivanov (1942–2004), who was a Senior Member of the IEEE.

REFERENCES

[1] *"IPC TM-650 2.5.5.5, Test Methods Manual: Stripline Test for Permittivity and Loss Tangent at X-Band"* IPC, Northbrook, IL, Mar. 1998 [Online]. Available: http://www.ipc.org/html/fsstandards.htm

[2] E. Drake, R. R. Boix, M. Horno, and T. K. Sarkar, "Effect of dielectric anisotropy on the frequency behavior of microstrip circuits," *IEEE Trans. Microw. Theory Tech.*, vol. 48, no. 8, pp. 1394–1403, Aug. 2000.

[3] S. A. Ivanov and P. I. Dankov, "Estimation of microwave substrate materials anisotropy," *J. Elect. Eng. (Slovakia)*, vol. 53, no. 9s, pp. 93–95, 2002.

[4] P. Dankov, S. Kamenopolsky, and V. Boyanov, "Anisotropic substrates and utilization of microwave simulators," in *Proc. 14th Microcoll*, Budapest, Hungary, Sep. 2003, pp. 217–220.

[5] S. A. Ivanov and V. N. Peshlov, "Ring-resonator method—Effective procedure for investigation of microstrip line," *IEEE Microw. Wireless Compon. Lett.*, vol. 13, no. 7, pp. 244–246, Jul. 2003.

[6] P. Dankov, S. Kolev, and S. Ivanov, "Measurement of dielectric and magnetic properties of thin nano-particle absorbing films," in *Proc. 17th EM Field Mater.*, Warsaw, Poland, May 2004, pp. 89–93.

[7] D. G. Bodnar and H. L. Bassest, "Analysis of an anosotropic dielectric radome," *IEEE Trans. Antennas Propag.*, vol. AP-23, no. 11, pp. 841–846, Nov. 1975.

[8] P. I. Dankov and S. A. Ivanov, "Two-resonator method for measurement of dielectric constant anisotropy in i.e., layer thin films, substrates and antenna radomes," in *Proc. 34th Eur. Microw. Conf.*, Amsterdam, The Netherlands, Oct. 2004, pp. 753–756.

[9] J. Baker-Jarvis, R. G. Geyer, J. H. Grosvenor, M. D. Janezic, C. A. Jones, B. Riddle, C. M. Weil, and J. Krupka, "Dielectric characterization of low-loss materials. A comparison of techniques," *IEEE Trans. Dielect. Electr. Insul.*, vol. 5, no. 4, pp. 571–577, Aug. 1998.

[10] Radio-Freq. Technol. Div., Electron. Elect. Eng. Lab., NIST, Boulder, CO, Electromagnetic properties of materials 2005 [Online]. Available: http://www.boulder.nist.gov/div813/emagprop.htm

[11] EMMA-Club, Nat. Phys. Lab., Middlesex, U.K., RF and microwave dielectric and magnetic measurements, electro-magnetic material characterization 2005 [Online]. Available: http://www.npl.co.uk/electromagnetic/rfmffnewcal/rfmwdielectrics.html

[12] W. E. Courtney, "Analysis and evaluation of a method of measuring the complex permittivity and permeability of microwave insulators," *IEEE Trans. Microw. Theory Tech.*, vol. MTT-18, no. 8, pp. 476–485, Aug. 1970.

[13] G. Kent, "An evanescent-mode tester for ceramic dielectric substrates," *IEEE Trans. Microw. Theory Tech.*, vol. 36, no. 10, pp. 1451–1454, Oct. 1988.

[14] E. Vanzura, R. Geyer, and M. Janezic, The NIST 60-millimeter diameter cylindrical cavity resonator: Performance for permittivity measurements NIST, Boulder, CO, Tech. Note 1354, Aug. 1993.

[15] M. D. Janezic and J. Baker-Jarvis, "Full-wave analysis of a split-cylinder resonator for nondestructive permittivity measurements," *IEEE Trans. Microw. Theory Tech.*, vol. 47, no. 10, pp. 2014–2020, Oct. 1999.

[16] X. Zhao, C. Liu, and L. C. Shen, "Numerical analysis of a TM_{010} cavity for dielectric measurements," *IEEE Trans. Microw. Theory Tech.*, vol. 40, no. 10, pp. 1951–1958, Oct. 1992.

[17] J. Baker-Jarvis and B. F. Riddle, Dielectric measurement using reentrant cavity NIST, Boulder, CO, Tech. Note 1384, Nov. 1996.

[18] J. Krupka, D. Cros, M. Aubourg, and P. Giullion, "Study of whispering gallery modes in anisotropic single-crystal dielectric resonators," *IEEE Trans. Microw. Theory Tech.*, vol. 42, no. 1, pp. 56–61, Jan. 1994.

[19] J. Krupka, K. Derzakowski, A. Abramowicz, M. Tobar, and R. G. Gayer, "Complex permittivity measurement of extremely low-loss dielectric materials using whispering gallery modes," in *IEEE MTT-S Int. Microw. Symp. Dig.*, 1997, pp. 1347–1350.

[20] V. N. Egorov, V. L. Masalov, Y. A. Nefyodov, A. F. Shevchun, M. R. Trunin, V. E. Zhitomirsky, and M. McLean, "Dielectric constant, loss tangent, and surface resistance of PCB materials at K-band frequencies," *IEEE Trans. Microw. Theory Tech.*, vol. 53, no. 2, pp. 627–635, Feb. 2005.

[21] M. Olyphant, Jr., "Measuring anisotropy in microwave substrates," in *IEEE MTT-S Int. Microw. Symp. Dig.*, 1979, pp. 91–93.

[22] R. F. Harrington, *Time–Harmonic Electromagnetic Field*. New York: McGraw-Hill, 1961, ch. 5.

[23] M. D. Janezic, E. F. Kuester, and J. Baker-Jarvis, "Broadband permittivity and loss tangent measurements using a split-cylinder resonator," in *Proc. IMAPS Ceramic Interconnect Technol. Conf.*, Denver, CO, 2003 [Online]. Available: http://www.boulder.nist.gov/div813/rfelec/properties/Pages/publications.html

[24] B. C. Wadell, *Transmission-Line Design Handbook*. Boston, London: Artech House, 1991, ch. 2.

[25] Y. Kobayashi and M. Katoh, "Microwave measurement of dielectric properties of low-loss materials by the dielectric rod resonator method," *IEEE Trans. Microw. Theory Tech.*, vol. MTT-33, no. 7, pp. 586–592, Jul. 1985.

[26] A. P. Mourachkine and A. R. F. Barel, "Microwave measurement of surface resistance by the parallel-plate dielectric resonator method," *IEEE Trans. Microw. Theory Tech.*, vol. 43, no. 3, pp. 544–551, Mar. 1995.

[27] Y. Kobayashi and H. Yoshikawa, "Microwave measurements of surface impedance of high-Tc superconductors using two modes in a dielectric rod resonator," *IEEE Trans. Microw. Theory Tech.*, vol. 46, no. 12, pp. 2524–2530, Dec. 1998.

[28] TEKLAM, Commercial grade panels. [Online]. Available: http://www.teklam.com/teklam_commercial_panels.html

[29] PARABEAM, 3-D glass fabrics. [Online]. Available: http://www.parabeam.nl/Product/

Plamen I. Dankov (M'99) was born in Pleven, Bulgaria, in 1955. He received the M.S. degree and Ph.D. degree in microwave physics (planar microwave gyrotropic structures and devices) from Sofia University, Sofia, Bulgaria, in 1980 and 1988, respectively.

Since 1992, he has been a Lecturer and Associate Professor with the Department of Radio-Physics and Electronics, Sofia University. He is currently Head of the Department of Radio-Physics and Electronics. His educational activity includes the reading of courses in the area of microwave technique and measurements, microwave integrated circuits and electronics, microwave gyrotropic media, electromagnetic design and simulation tools, and mobile communication systems. He is engaged also in lecturing on general electronics for physicists. In 1997, he began work as a scientific consultant with Ray Sat BG Ltd. He has authored or coauthored over 60 scientific and popular publications. His research interests and activities include design of microwave gyrotropic devices, microwave material characterization, electromagnetic compatibility (EMC) problems (determination of safety zones and standards), microwave "in-fixture" measurements and deembedding procedures, 3-D electromagnetic simulations, etc.

Dr. P. Dankov is member of the Bulgarian Union of Physicists.

View publication stats